[CANCER RESEARCH 64, 9035–9040, December 15, 2004]

Inhibition of Chk1 by CEP-3891 Accelerates Mitotic Nuclear Fragmentation in Response to Ionizing Radiation

Randi G. Syljuåsen,[1] Claus Storgaard Sørensen,[1] Jesper Nylandsted,[2] Claudia Lukas,[1] Jiri Lukas,[1] and Jiri Bartek[1]

[1]Department of Cell Cycle and Cancer and [2]Apoptosis Laboratory, Institute of Cancer Biology, Danish Cancer Society, Copenhagen, Denmark

ABSTRACT

The human checkpoint kinase Chk1 has been suggested as a target for cancer treatment. Here, we show that a new inhibitor of Chk1 kinase, CEP-3891, efficiently abrogates both the ionizing radiation (IR)-induced S and G_2 checkpoints. When the checkpoints were abrogated by CEP-3891, the majority (64%) of cells showed fragmented nuclei at 24 hours after IR (6 Gy). The formation of nuclear fragmentation in IR-treated human cancer cells was directly visualized by time-lapse video microscopy of U2-OS cells expressing a green fluorescent protein-tagged histone H2B protein. Nuclear fragmentation occurred as a result of defective chromosome segregation when irradiated cells entered their first mitosis, either prematurely without S and G_2 checkpoint arrest in the presence of CEP-3891 or after a prolonged S and G_2 checkpoint arrest in the absence of CEP-3891. The nuclear fragmentation was clearly distinguishable from apoptosis because caspase activity and nuclear condensation were not induced. Finally, CEP-3891 not only accelerated IR-induced nuclear fragmentation, it also increased the overall cell killing after IR as measured in clonogenic survival assays. These results demonstrate that transient Chk1 inhibition by CEP-3891 allows premature mitotic entry of irradiated cells, thereby leading to accelerated onset of mitotic nuclear fragmentation and increased cell death.

INTRODUCTION

In response to DNA-damaging agents such as ionizing radiation (IR), cells activate cell cycle checkpoints to delay cell cycle progression. Recently, much progress has been made toward understanding the signaling cascades responsible for induction of these checkpoints. The aim of the present study was to develop new tools to abrogate IR-induced checkpoints and explore the effects of checkpoint abrogation on cell survival.

Recent data showed that human Chk1 is required for both the IR-induced rapid S and G_2 checkpoints (1–4). Chk1, which was known to be involved in the response to ultraviolet light and replication stress (5, 6), therefore plays a much more important role in the cellular response to IR than previously thought. We and others found that Chk1 controls the S-phase checkpoint by directly phosphorylating Cdc25A (3, 4), a human phosphatase that activates the S-phase promoting cyclin-dependent kinase (Cdk) 2 (7). When Chk1 is inhibited, the Cdc25A phosphatase and, consequently, Cdk2 kinase activity are not down-regulated after IR, and the S-phase checkpoint is impaired (3, 4). Chk1 is believed to control the G_2 checkpoint via phosphorylation-mediated negative regulation of Cdc25A, Cdc25C, and Cdc25B (4, 8). All three members of the Cdc25 family of phosphatases contribute to activation of the M phase promoting Cdk1 (9–11).

Previous studies have suggested that compounds that abrogate the G_2 checkpoint will increase the sensitivity of human cancer cells to the cytotoxic effects of IR and chemotherapeutic drugs (reviewed in ref. 12). Cancer cells, which commonly lack normal G_1 checkpoint control and may therefore rely more on the G_2 checkpoint, could likely be more affected by G_2 checkpoint abrogation than normal cells (13, 14). The classic compounds known to abrogate the G_2 checkpoint are caffeine, an inhibitor of the ATR/ATM kinases (15, 16), and UCN-01, a protein kinase C inhibitor that, in addition to other kinases, also inhibits Chk1 (17). However, although these drugs inhibit the G_2 checkpoint and increase radiosensitivity, the relationship between checkpoint abrogation and radiosensitivity is not clear (18). For example, genetic manipulations of a checkpoint-defective and radiosensitive cell line could restore the checkpoint defects without affecting radiosensitivity (19). Moreover, caffeine was shown to inhibit DNA repair (20), and its radiosensitizing effect may be due to defective repair rather than checkpoint abrogation. UCN-01, which was originally synthesized as a staurosporine analog, caused apoptosis in human cancer cells when combined with IR (21).

Cell death in response to IR is best measured as a loss of reproductive integrity (22). The predominant death mechanism for most solid tumors of nonhematopoetic origin is mitosis-linked death, which is characterized by the appearance of cells with multiple nuclear fragments or micronuclei (23–27). IR-induced micronucleus formation requires progression through mitosis and is due to IR-induced chromosome aberrations (24, 26). Cell death under such circumstances occurs as a consequence of chromosomal aberrations, which may finally result in loss of transcription of essential genes after cells have passed through mitosis (26–28).

Given that Chk1 is emerging as a major regulator of IR-induced checkpoints, we wanted to explore the effects of a new specific Chk1 inhibitor, CEP-3891 (3), on checkpoint activation and cell death. We show that CEP-3891 efficiently abrogates the IR-induced S and G_2 checkpoints, which results in an accelerated onset of nuclear fragmentation when IR-treated cells progress prematurely through mitosis. Treatment with CEP-3891 also increases the radiosensitivity of human cells as measured by clonogenic survival assays. These results provide new insights into cellular consequences of checkpoint abrogation by inhibition of Chk1.

MATERIALS AND METHODS

Cell Lines, Drugs, and Irradiation. Human U2-OS and U2-OS-VP16 (a subclone of U2-OS) osteosarcoma cell lines were grown in Dulbecco's modified Eagle's medium (DMEM) with 10% fetal bovine serum. U2-OS VP16 cells were transfected with H2B-GFP (Clontech, Palo Alto, CA) and selected in DMEM containing blastidicin (5 μg/μL) and G418 (400 μg/μL). The CEP-3891 Chk1 inhibitor was provided by Cephalon Inc. and used at a concentration of 500 nmol/L. IR was delivered by X-ray generator (Pantak, Berkshire, United Kingdom; HF160; 150kV; 15 mA; dose rate, 2.18 Gy/min).

Antibodies and Immunochemistry. Immunoblotting, immunoprecipitation, and *in vitro* kinase assays have been described previously (3). Recombinant active Chk1 and antibody 06--570 to phosphorylated histone H3 were purchased from Upstate Biotechnology (Lake Placid, NY). Antibodies to cyclin A (sc-751), cyclin B1 (sc-245), and Cdk2 (sc-163) were purchased from Santa Cruz Biotechnology (Santa Cruz, CA), and antibody to Cdk-1 (Ab-1)

Received 7/10/04; revised 10/1/04; accepted 10/19/04.

Grant support: Danish Cancer Society, Danish Medical Research Council, Alfred's Benzon's Fund, the EU, and John and Birthe Meyer Foundation.

The costs of publication of this article were defrayed in part by the payment of page charges. This article must therefore be hereby marked *advertisement* in accordance with 18 U.S.C. Section 1734 solely to indicate this fact.

Note: Supplementary data for this article can be found at Cancer Research Online (http://cancerres.aacrjournals.org). Present address for C. Storgaard Sørensen is Biotech Research and Innovation Centre, Copenhagen, Denmark.

Requests for reprints: Jiri Bartek, Department of Cell Cycle and Cancer, Institute of Cancer Biology, Strandboulevarden 49, 2100 Copenhagen, Denmark. Phone: 45-35257357; Fax: 45-35257721; E-mail: bartek@biobase.dk.

©2004 American Association for Cancer Research.

Downloaded from cancerres.aacrjournals.org on September 18, 2021. © 2004 American Association for Cancer Research.

was purchased from Calbiochem (San Diego, CA). Fluorescein-conjugated antirabbit immunoglobulin (Alexa Fluor 488 goat anti-IgG) was purchased from Molecular Probes (Eugene, OR).

Flow Cytometry. To assay cell cycle distribution by DNA content, trypsinized cells were fixed in 70% EtOH, stained with 0.1 mg/mL propidium iodide, and analyzed by a FACSCalibur flow cytometer (BD Biosciences, Stockholm, Sweden) using Cellquest software. For two-parameter flow cytometry analysis to assay the number of mitotic cells (19), fixed cells were incubated with PBS/0.25% Triton X-100 for 15 minutes on ice and stained with antibody to phosphorylated histone H3 (1:500) for 1 hour at room temperature, followed by a 30-minute incubation with fluorescein conjugated antirabbit immunoglobulin antibody (1:500). Cells were then stained with propidium iodide and analyzed as described above.

Inhibition of DNA Synthesis. Inhibition of DNA synthesis was assessed by standard [^{3}H]thymidine/[^{14}C]thymidine assay as described previously (3).

Fluorescent Time-Lapse Videomicroscopy. U2-OS-GFP-H2B cells were grown in Lab-Tek chambered cover glass (Nalge Nunc International, Rochester, NY) and incubated at 37°C in phenol red-free, CO_2-independent medium (Invitrogen, Paisley, United Kingdom) overlaid with mineral oil. Fluorescence and differential interference contrast images were acquired using a charge-coupled device camera (CoolSnap/VP; Roper Scientific, Tuscon, AZ) mounted on an Axiovert 200 microscope [Zeiss; 12 frames per hour; exposure times, 10 (differential interference contrast) and 15 milliseconds (fluorescence); ×40 objective (unless otherwise stated in the figure legend)] and subsequently processed by the Metamorph software package.

Nuclear Staining. Cells cultured on glass coverslips were treated with CEP-3891 (0 or 500 nmol/L), exposed to IR (0 or 6 Gy) for a time period specified in the figure legends, and stained by ToPro3 (Molecular Probes, Eugene, OR) to mark nuclear DNA. Confocal images were obtained by using a Zeiss 510 laser scanning microscope (Axiovert) and operated by LSM510 software. For quantification of nuclear fragmentation, at least 200 cells were scored for each sample.

Hoechst/Sytox Staining to Detect Apoptosis. Cultured U2-OS-VP16 cells were incubated with a mixture of the membrane-permeable dye Hoechst 33342 (500 ng/mL) and the membrane-impermeable dye Sytox green (500 nmol/L) for 5 minutes at 37°C, and images were obtained using an epifluorescence microscope as described previously (29).

Clonogenic Survival Assays. Between 250 and 2,000 cells (depending on radiation dose to yield 50–100 colonies per dish) were seeded to 6-cm–diameter dishes, incubated for 20 to 24 hours, and treated with CEP-3891 (0 or 500 nmol/L) and IR (0, 2, 4, or 6 Gy). After 24 hours, the medium was removed, cells were washed once with PBS, and regular DMEM was added. Cells were cultivated for another 12 to 13 days and then stained with crystal violet. Colonies containing more than 50 cells were scored as survivors. Survival fractions were calculated in each experiment as the average cloning efficiency (from three parallel dishes) after IR divided by the average cloning efficiency for nonirradiated cells. The cloning efficiencies for nonirradiated U2–0S-VP16 cells were about 0.6 and 0.5 in the absence and presence of CEP-3891 (500 nmol/L, 24 hours), respectively.

Caspase Activity. To measure total caspase activity, subconfluent cells were treated with an extraction buffer [250 mmol/L sucrose, 20 mmol/L HEPES, 10 mmol/L KCl, 1.5 mmol/L $MgCl_2$, 1 mmol/L EDTA, 1 mmol/L EGTA, and 1 mmol/L pefablock (pH 7.5)] containing 200 μg/mL digitonin for 15 minutes on ice. The effector caspase activities were estimated by adding 1 volume of 20 μmol/L N-acetyl-Asp-Glu-Val-Asp-7-amino-trifluoromethyl-coumarin (Biomol, Plymouth, PA) in caspase reaction buffer [100 mmol/L HEPES, 20% glycerol, 0.5 mmol/L EDTA, 0.1% 3-[(3-cholamidopropyl)-dimethylammonio]-1-propanesulfonic acid, 5 mmol/L dithiothreitol, and 1 mmol/L pefablock (pH 7.5)]. The V_{max} of the liberation of AFC (excitation, 400 nm; emission, 489 nm) was measured over 20 minutes at 30°C with a Spectramax Gemini fluorometer (Molecular Devices, Sunnyvale, CA). Lactate dehydrogenase activity of the cytosol determined by a cytotoxicity detection kit (Roche A/S Diagnostic, Hvidovre, Denmark) was used as an internal standard to which protease activities were normalized.

RESULTS

CEP-3891 Abrogates the Ionizing Radiation-Induced S and G_2 Checkpoints. CEP-3891, a new inhibitor of Chk1 kinase, is more specific than existing Chk1 inhibitors such as UCN-01 (ref. 3; see Supplementary Table of Ref. 3 for *in vitro* inhibitory effects of Cep-3891 on a number of human kinases). Here, we first verified that CEP-3891 can inhibit the activity of recombinant Chk1 *in vitro* (Fig. 1*A*). Next, we examined whether this inhibitor could abrogate the *in vivo* induction of the Chk1-dependent S and G_2 checkpoints in response to IR. As seen in Fig. 1*B*, *bottom panels*, CEP-3891 significantly abrogated the rapid IR-induced G_2 checkpoint measured at 1 hour after 6 Gy. CEP-3891 also caused an increased entry of cells from G_2 to M phase in the absence of IR (Fig. 1*B*, *top panels*), consistent with a role for Chk1 in control of G_2 to M progression in both the presence and absence of IR. Furthermore, CEP-3891 efficiently abrogated the delayed IR-induced G_2 checkpoint, which was

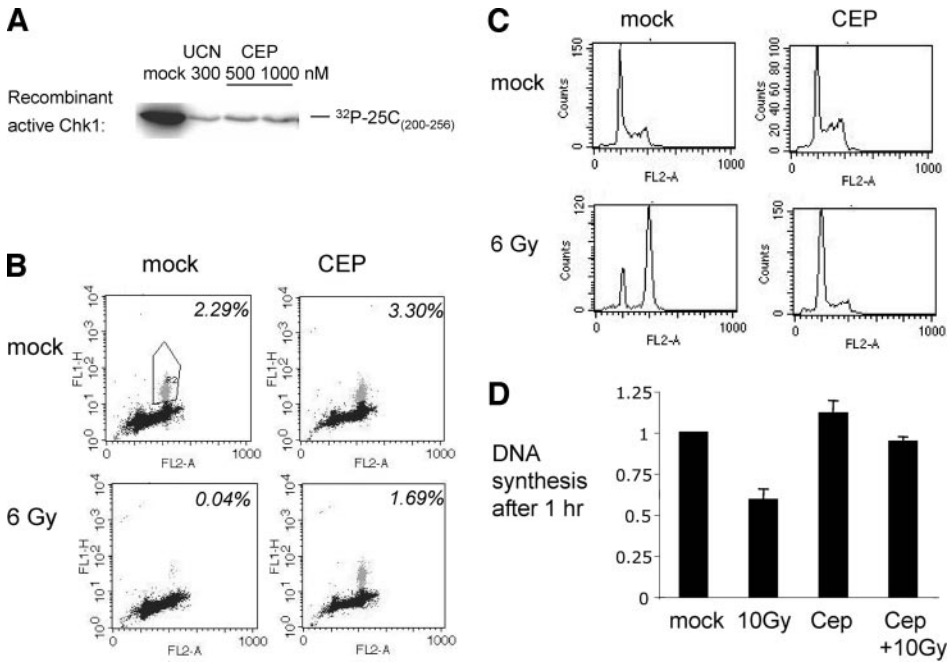

Fig. 1. Chk1 inhibitor CEP-3891 abrogates the IR-induced S and G_2 checkpoints. *A*. CEP-3891 inhibits Chk1 kinase activity. *In vitro* kinase assays are shown for recombinant active Chk1 (*mock*) and with UCN-01(300 nmol/L) or CEP-3891 (500 or 1,000 nmol/L) added to the kinase reaction. A fragment of Cdc25C containing residue Ser^{216} [GST-Cdc25C$_{(200–256)}$] was used as a substrate. *B*. CEP-3891 abrogates the rapid IR-induced G_2 checkpoint. Histone H3 phosphorylation (*FL1-H*) *versus* DNA content (*FL2-A*) is shown in U2-OS cells at 1 hour after the indicated treatment. The results of a representative experiment are shown. *Numbers* indicate the percentage of mitotic cells. *C*. CEP-3891 abrogates the delayed IR-induced G_2 checkpoint. DNA histograms are shown for U2–0S cells at 20 hours after the indicated treatments. *D*. CEP-3891 (*Cep*; 500 nmol/L) abrogates the IR-induced S-phase checkpoint. DNA synthesis at 1 hour after treatment is shown. *Error bars* are SEs of three independent experiments (performed with two parallel dishes for each data point in each experiment).

Downloaded from cancerres.aacrjournals.org on September 18, 2021. © 2004 American Association for Cancer Research.

assayed at 20 hours after 6 Gy (Fig. 1*C*). When nocodazole was added to the culture medium, the CEP-3891–treated and CEP-3891 + 6 Gy-treated cells accumulated at mitosis, demonstrating that CEP-3891–treated cells were cycling over the time course of this experiment (data not shown). Consistent with our previous report (3), CEP-3891 also abrogated the IR-induced S-phase checkpoint and slightly increased the rate of DNA synthesis in the absence of IR (Fig. 1*D*).

To further investigate how CEP-3891 abrogates the S and G_2 checkpoints, we assayed the activities of major cell cycle-regulating kinases in a time course after CEP-3891 and IR treatment (Fig. 2). A transient down-regulation of cyclin A- and B-associated kinase activities was found in IR-treated cells (Fig. 2*A* and *B*, *6 Gy*), consistent with the induction of the S and G_2 phase checkpoints (Fig. 1) and previous reports (see refs. 3, 4, and 23). Addition of CEP-3891 in the absence of IR caused a marked transient increase of these kinase activities (Fig. 2*A* and *B*, *CEP*), consistent with the effects of CEP-3891 on cell cycle progression seen in Fig. 1*B* and *D*. Similar effects were seen for cyclin E- associated kinase activity (data not shown). When U2-OS cells were treated with CEP-3891 in addition to IR, the IR-induced down-regulation of cyclin A- and B-associated kinase activities was abrogated (Fig. 2*A* and *B*, *CEP + 6 Gy*), consistent with the abrogation of the S and G_2 checkpoints (Fig. 1).

CEP-3891 Accelerates Ionizing Radiation-Induced Mitotic Fragmentation. Having established that addition of CEP-3891 would impair both the S and G_2 checkpoints, we explored the effects of CEP-3891 on IR-induced cell death (Fig. 3). The predominant type of IR-induced cell death of most solid tumors is mitosis-linked death, which is manifested by the appearance of nuclear fragmentation (or micronucleus formation after low radiation doses), occurring as a consequence of passage of IR-treated cells through mitosis (23–26). We first tested whether our IR-treated U2-OS cells underwent nuclear fragmentation (Fig. 3*A*). As evident from the results, U2-OS cells irradiated with 6 Gy underwent massive nuclear fragmentation after exit from the G_2 checkpoint (Fig. 3*A*, 48 and 72 hours). The majority of the cells with nuclear fragmentation had DNA content close to G_1-phase cells (Fig. 3*A*, DNA histograms), indicating that although

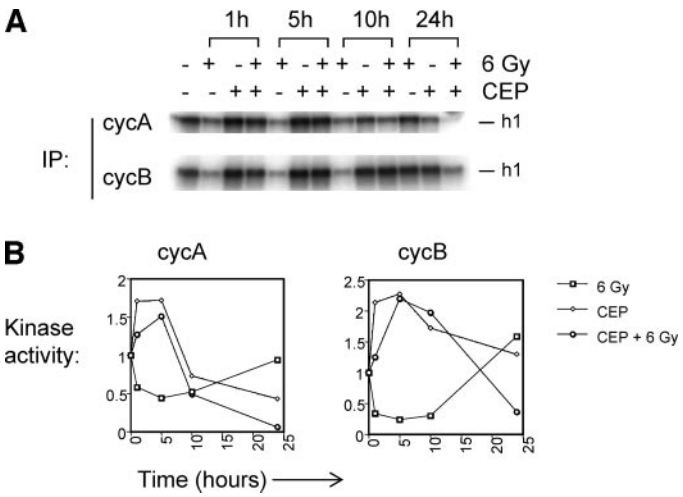

Fig. 2. CEP-3891 abrogates the IR-induced down-regulation of major cell cycle-regulating kinases. *A*, *in vitro* kinase activities in extracts from U2–0S cells treated with CEP-3891 and/or IR. Kinase complexes were immunoprecipitated (*IP*) from 40 and 20 μg of total cell extracts of U2–0S cells by antibodies to cyclin A (*cycA*) and cyclin B (*cycB*), respectively, and the corresponding *in vitro* kinase activities were measured with histone H1 as a substrate. The results of a representative experiment are shown. *B*, quantification of the *in vitro* kinase activities shown in *A*. Results are shown for each treatment relative to the activity of nontreated cells. The decline in activities at late time points after treatment with CEP-3891 and IR reflects passage through mitosis and the corresponding cyclin degradation.

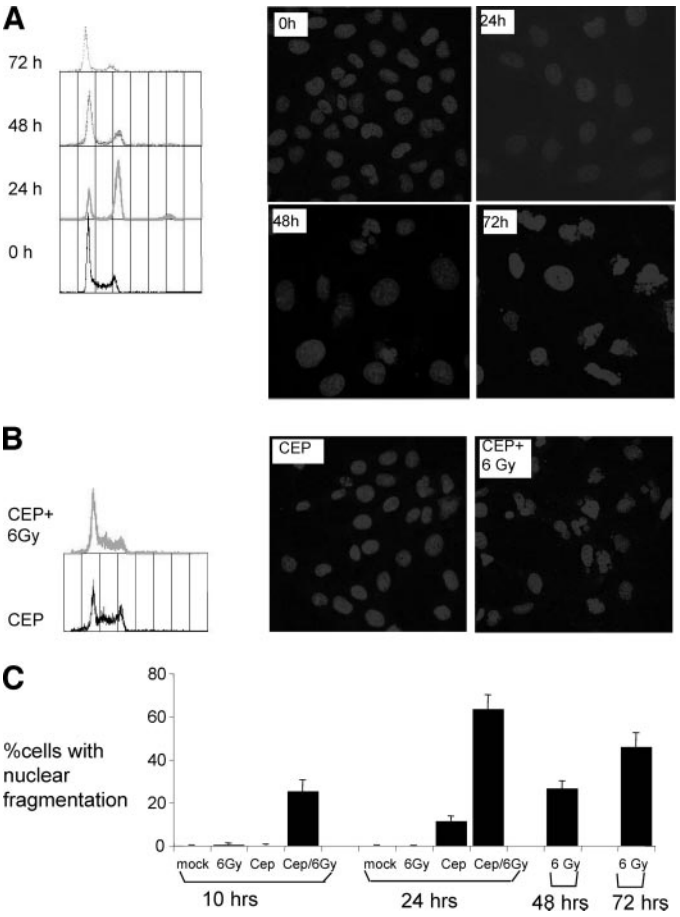

Fig. 3. Chk1 inhibition by CEP-3891 accelerates IR-induced nuclear fragmentation. *A*. IR-induced nuclear fragmentation occurs after exit from G_2 arrest. DNA histograms and images of cells stained with ToPro3 are shown at 0, 24, 48, and 72 hours after IR (6 Gy). *B*. When U2–0S cells were treated with CEP-3891 together with IR, massive nuclear fragmentation was evident at 24 hours. DNA histograms and pictures of ToPro3-stained cells are shown at 24 hours after treatment with CEP-3891 (500 nmol/L) and CEP-3891 (500 nmol/L) + IR (6 Gy). *C*. Quantification of cells with nuclear fragmentation is shown after treatment with IR (6 Gy), CEP-3891 (500 nmol/L), or CEP-3891 + IR. *Error bars* are SEs of three independent experiments. At least 200 cells were counted for each data point in each experiment.

the nucleus had split into several subnuclear fragments, the total amount of DNA of each daughter cell was close to normal G_1 phase cells. A similar pattern of IR-induced nuclear fragmentation has been reported in HeLa cells (23), and in U2-OS cells irradiated with 10 Gy (30). When the IR-induced S and G_2 checkpoints were abrogated by addition of CEP-3891, massive nuclear fragmentation was seen already at 24 hours after IR (Fig. 3*B*). Quantification of the number of cells with nuclear fragmentation in a time course showed that treatment with CEP-3891 in addition to IR accelerated the time for onset of nuclear fragmentation compared with treatment with IR alone (Fig. 3*C*). Acceleration of mitotic cell death by CEP-3891 appeared to be a more general response rather than a specific phenomenon limited to U2-OS cells because other cell types, including normal human fibroblasts, also showed a significant fraction of cells with nuclear fragmentation at 24 hours after treatment with CEP-3891 and IR (data not shown).

Time-Lapse Studies of Formation of Nuclear Fragmentation. Although the time for onset of nuclear fragmentation after IR correlated with the time of progression through mitosis (Fig. 3; ref. 23), and abnormal mitotic figures were present (data not shown; ref. 23), no direct and dynamic visualization of the process of formation of cells with nuclear fragmentation has thus far been reported. We generated

Downloaded from cancerres.aacrjournals.org on September 18, 2021. © 2004 American Association for Cancer Research.

a human model system for a constitutive expression of green fluorescent protein (GFP)-tagged histone H2B (31) to directly visualize chromosomal dynamics in the absence and presence of CEP-3891 by time-lapse fluorescent video microscopy (Fig. 4). These experiments revealed that U2-OS-H2B-GFP cells underwent normal chromosome segregation in the absence of IR or CEP-3891 treatment (Fig. 4*A*; Supplementary Fig. 1). In response to IR (6 Gy), mitotic cells appeared after exit from a prolonged G_2 checkpoint arrest. The results of videorecording of arbitrary selected mitotic cells that appeared at 40 to 50 hours after IR clearly demonstrated that nuclear fragmentation was a result of defective chromosome segregation in mitosis (Fig. 4*B*; Supplementary Fig. 2). When CEP-3891 was added together with IR, cells were entering mitosis prematurely without induction of the S and G_2 checkpoints, and mitotic cells were present at all times within the first 24 hours after IR. Similar to the delayed process of nuclear fragmentation after exit from G_2 arrest in the IR-treated cells (Fig. 4*B*), the more rapid nuclear fragmentation occurring when the checkpoints were abrogated by CEP-3891 also reflected defective chromosome segregation in mitosis (Fig. 4*C*; Supplementary Fig. 3).

Nuclear Fragmentation Is Not a Result of Apoptosis. Nuclear fragmentation is often associated with apoptotic cell death (32). To explore whether the mitotic induction of nuclear fragmentation was related to apoptosis, we measured the extent of caspase activity in U2-OS cells at 12, 24, and 48 hours after IR and CEP-3891 treatment (Fig. 5*A*). Although massive nuclear fragmentation was found in U2-OS cells treated with IR + CEP-3891 at 24 hours, no significant increase in caspase activity was found at 12 or 24 hours (Fig. 5*A*), indicating that nuclear fragmentation was not a result of classical apoptosis. However, a small increase in caspase activity was found at 48 hours after treatment with CEP-3891 and IR, suggesting that cells died at later times at least partly via apoptosis (Fig. 5*A*).

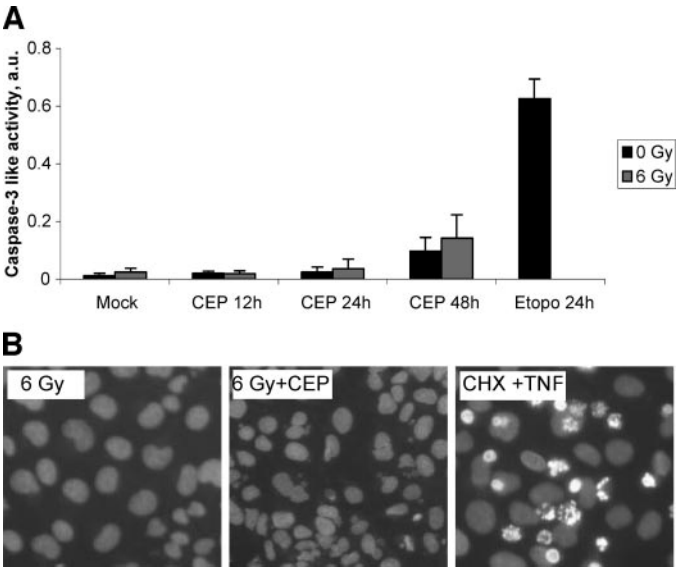

Fig. 5. *A*, caspase-3–like activity measured and expressed in arbitrary units (*a.u.*) at 12, 24, and 48 hours after treatment (mock, 6 Gy, 500 nmol/L CEP-3891, or 6 Gy + CEP-3891) of U2-OS cells. Etoposide (100 μmol/L) was included as a positive control. *B*, Hoechst/Sytox green staining at 24 hours after treatment with 6 Gy and/or 500 nmol/L CEP-3891. Treatment with cycloheximide (*CHX*) and human tumor necrosis factor α (*TNF*) was included as positive control (1 μg/mL cycloheximide for 2 hours followed by 10 ng/mL human tumor necrosis factor α for an additional 16 hours).

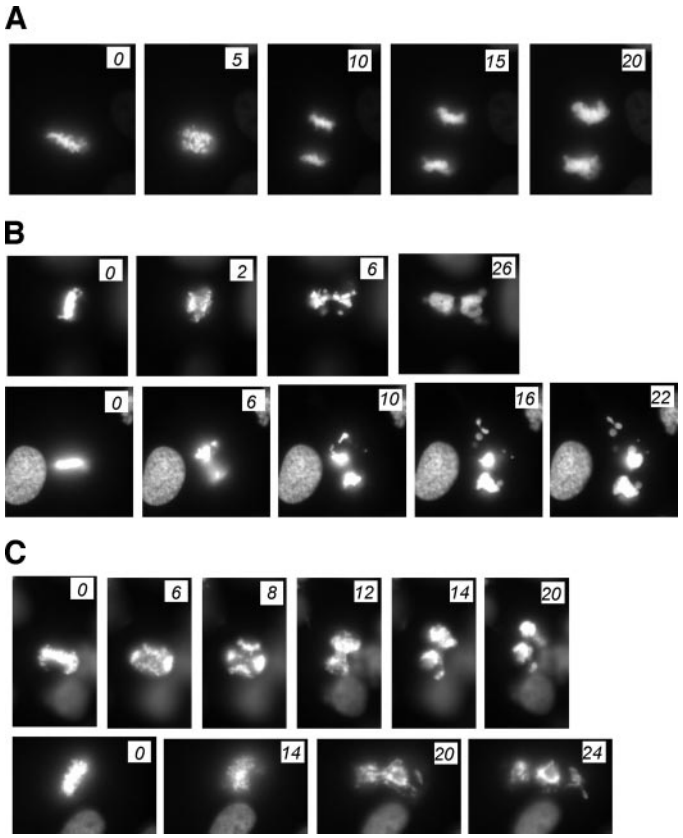

Fig. 4. Nuclear fragmentation occurs as a result of defective chromosome segregation in mitosis. *A*, live cell imaging of nontreated mitotic U2–0S-H2B-GFP cells. Arbitrary mitotic cells were selected and processed for time-lapse videomicroscopy. A representative image gallery is shown. *Numbers* indicate time (in minutes) relative to the first image in the series. *B*, live cell imaging of mitotic U2-OS-H2B-GFP cells after IR (6 Gy). Arbitrary mitotic cells were selected between 40 and 50 hours after IR and processed for time-lapse videomicroscopy (30 frames per hour). *C*, live cell imaging of mitotic U2-OS-H2B-GFP cells after treatment with CEP-3891 (500 nmol/L) + IR (6 Gy). Arbitrary mitotic cells were selected between 5 and 15 hours after treatment and processed for time-lapse videomicroscopy (30 frames per hour).

Furthermore, nuclear fragmented cells at 24 hours after treatment with CEP-3891 and IR did not show the characteristic nuclear condensation (Fig. 5*B*), which would have been expected to accompany apoptosis (32). The majority of CEP-3891 and IR-treated cells also did not stain with the membrane-impermeable dye Sytox green (Fig. 5*B*; data not shown); therefore, these cells were not likely to be at late stages of apoptosis. Taken together, these results show that the massive nuclear fragmentation after inhibition of Chk1 and IR is not a result of apoptosis.

CEP-3891 Increases Overall Cell Killing after Ionizing Radiation. Finally, we explored the effect of CEP-3891 on the extent of overall cell killing after IR as measured in clonogenic survival assays (Fig. 6*A*). The results showed that CEP-3891 sensitized U2-OS cells to the cytotoxic effects of IR (Fig. 6*A*), to an extent nearly comparable with the sensitization obtained by 2 mmol/L caffeine, an established radiosensitizer (15).

DISCUSSION

The results of this study suggest that inhibition of Chk1 abrogates the IR-induced S and G_2 checkpoints, followed by premature mitotic entry, defective chromosome segregation, and nuclear fragmentation (Fig. 6*B*). In the absence of CEP-3891, IR-treated cells arrest in G_2 for several hours before they eventually enter mitosis. After a relatively high dose of IR, such as 6 Gy, most of the cells that eventually enter mitosis contain so much chromosome damage that defective chromosome segregation and nuclear fragmentation occur, followed by cell death. Most cells that arrest in G_2 after 6 Gy therefore contain irreparable lesions; nevertheless, the cells are eventually released from the checkpoint and progress through mitosis. Therefore, a process of

Downloaded from cancerres.aacrjournals.org on September 18, 2021. © 2004 American Association for Cancer Research.

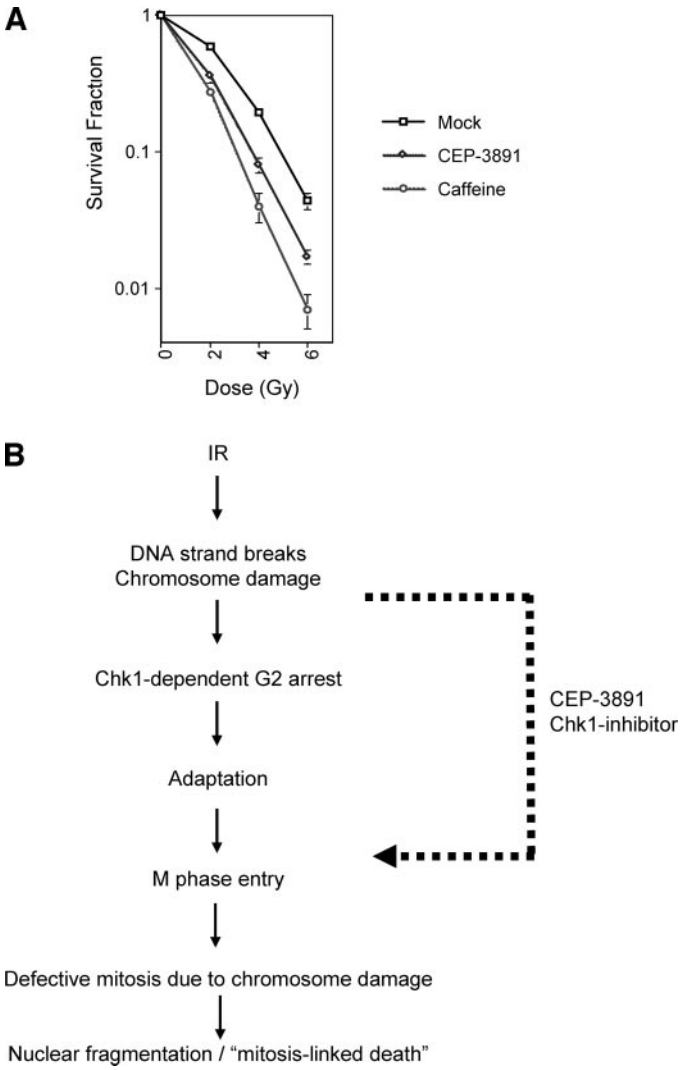

Fig. 6. *A*. CEP-3891 increases overall cell killing after IR as measured in clonogenic assays. Clonogenic assays of IR-treated U2-OS cells with addition of CEP-3891 (500 nmol/L) or caffeine (2 mmol/L) were performed as described in Materials and Methods. Results shown are the average of three to four independent experiments (each experiment was performed with three parallel dishes for each data point). *B*, model for accelerated IR-induced mitotic nuclear fragmentation by CEP-3891. IR causes DNA damage that leads to Chk1-dependent checkpoint arrest in S and G_2 phases. Cells with too much damage to survive after IR will arrest in G_2 phase for several hours and eventually exit from the G_2 checkpoint, likely after a process of adaptation to damage. When such cells progress through M phase, defective chromosome segregation occurs due to IR-induced chromosome damage, resulting in daughter cells with nuclear fragmentation. When the CEP-3891 Chk1 inhibitor is added together with IR, the S and G_2 checkpoints are abrogated, and cells enter prematurely into M phase without delay. In comparison with IR-treated cells, the CEP-3891 + IR-treated cells show similar but earlier and more common defective chromosome segregation in mitosis. Chk1 inhibition by CEP-3891 therefore accelerates the onset of IR-induced nuclear fragmentation.

adaptation to DNA damage likely occurs at the G_2 checkpoint (Fig. 6*B*). Adaptation to DNA damage has also been described in yeast (33) and *Xenopus* egg extracts (34).

Consistent with this concept, time-lapse studies have shown that both cells that survived and cells that died in clonogenic assays after IR (6 Gy), would transiently delay their cell cycle progression in the first cell cycle after IR (35). However, the cells that ended up as nonclonogenic (dead cells), on average, showed longer cell cycle delays compared with the clonogenic survivors (35). Thus, there may be two different processes that promote exit from the G_2 checkpoint: one that allows exit when the DNA damage is repaired, and another that eventually allows exit of cells with irreparable damage due to adaptation. The molecular mechanisms of these processes are unknown; however, dephosphorylation of the activating phosphorylations on Chk1 may be involved (36). It was also suggested that overaccumulation of cyclin B during checkpoint arrest due to a prolonged time in G_2 phase may contribute to cause exit from the G_2 checkpoint (23).

Another question is what kind of DNA lesion evokes the "signal" that triggers the prolonged G_2 checkpoint arrest. Unrejoined double-strand breaks (DSBs) and/or changes in chromatin structure are thought to trigger the rapid activation of ATM in response to DNA damage (37). Unrejoined DSBs likely contribute to the ATM-dependent S and G_2 checkpoints in the first few hours after IR. However, the majority of DSBs are rejoined within several hours after IR, and the prolonged G_2 checkpoint is independent of ATM (19, 38, 39). Although the signal for the prolonged G_2 checkpoint still could reflect the small proportion of remaining unrejoined DSBs, another possibility is that additional lesions are involved. IR-induced DSBs are converted into large-scale chromosomal damage [such as dicentrics, rings, and bridges (40)], which possibly could also be sensed by the cell's checkpoint machinery. In such a scenario, exit from G_2 checkpoint arrest could depend on complete rejoining of DSBs in addition to adaptation to large-scale chromosome damage.

We found that checkpoint abrogation by CEP-3891 increases cell cytotoxicity as measured in clonogenic survival assays (Fig. 6*A*). Thus, CEP-3891 not only accelerated IR-induced nuclear fragmentation but also caused an increased total number of dead cells. This result is consistent with a concept in which Chk1-mediated checkpoint arrest promotes repair of DNA damage before cells enter mitosis, in which defective chromosome segregation takes place if the damage was not properly repaired. It remains to be investigated whether Chk1 plays a direct role in regulating repair pathways after IR or whether Chk1 simply promotes repair by allowing more time before entry into mitosis.

We did not observe much cell death over the first 24 hours after CEP-3891 and IR treatment; however, caspase activity was slightly increased at 48 hours, indicating that cells died at later times at least partly via apoptosis (Fig. 5*A*). Future studies can address whether other death mechanisms such as necrosis or senescence are also involved. Previous extensive time-lapse studies have demonstrated that rat embryo cells transfected with c-myc underwent apoptosis after irradiated cells had divided once or several times (27, 41). This process was associated with formation of micronuclei in mitosis that preceded cell death (27), which may be analogous to our study, in which nuclear fragmentation in mitosis precedes cell death.

Chk1 is thought to regulate the S and G_2 checkpoints via phosphorylation of the human phosphatases Cdc25A, Cdc25B, and Cdc25C (4, 8). Although CEP-3891 efficiently abrogated the G_2 checkpoint, the level of Ser^{216} phosphorylation of Cdc25C was not altered by CEP-3891 treatment (data not shown). This was in contrast to the effects seen with UCN-01, which effectively reduced Ser^{216} phosphorylation under analogous experimental conditions (data not shown; ref. 17). Therefore the other phosphatases (Cdc25A and Cdc25B) may be more important than Cdc25C in control of the G_2 checkpoint. This finding is consistent with previous reports in which cells lacking Cdc25C showed a normal G_2 checkpoint response (11) and with the involvement of Cdc25A in the G_2 checkpoint (4, 10).

It has become increasingly clear that one of the general features of human cancer cells is defective DNA damage checkpoint control. It is therefore attractive to exploit new strategies to interfere with checkpoints in an attempt to find new cancer-specific treatments. Chk1 is one of several potential targets for checkpoint interference. Although Chk1 inhibition by UCN-01 showed promise as a cancer-selective treatment, particularly for cancer cells lacking p53 (42, 43), other studies failed to detect such specificity (44). It was proposed that more

Downloaded from cancerres.aacrjournals.org on September 18, 2021. © 2004 American Association for Cancer Research.

specific inhibition of Chk1 than that obtained with UCN-01 would likely be more effective (14). CEP-3891 was developed to make such a specific Chk1 inhibitor. The results of our study, using CEP-3891 to abrogate the IR-induced checkpoints, contribute to a better understanding of the cellular consequences of specific Chk1 inhibition. Additional studies of the effects of specific Chk1 inhibitors such as CEP-3891 on a broad panel of human cancer and normal cells, as well as *in vivo* studies in mice, will be needed to evaluate the true potential of Chk1 inhibition as a strategy for cancer treatment.

ACKNOWLEDGMENTS

We thank Cephalon Inc. for providing the CEP-3891 Chk1 inhibitor and Nicole Fehrenbacher for helpful technical advice.

REFERENCES

1. Xiao Z, Chen Z, Gunasekera AH, et al. Chk1 mediates S and G_2 arrests through Cdc25A degradation in response to DNA-damaging agents. J Biol Chem 2003;278:21767–73.
2. Gatei M, Sloper K, Sorensen C, et al. Ataxia-telangiectasia-mutated (ATM) and NBS1-dependent phosphorylation of Chk1 on Ser-317 in response to ionizing radiation. J Biol Chem 2003;278:14806–11.
3. Sorensen CS, Syljuasen RG, Falck J, et al. Chk1 regulates the S phase checkpoint by coupling the physiological turnover and ionizing radiation-induced accelerated proteolysis of Cdc25A. Cancer Cell 2003;3:247–58.
4. Zhao H, Watkins JL, Piwnica-Worms H. Disruption of the checkpoint kinase 1/cell division cycle 25A pathway abrogates ionizing radiation-induced S and G_2 checkpoints. Proc Natl Acad Sci USA 2002;99:14795–800.
5. Heffernan TP, Simpson DA, Frank AR, et al. An ATR- and Chk1-dependent S checkpoint inhibits replicon initiation following UVC-induced DNA damage. Mol Cell Biol 2002;22:8552–61.
6. Feijoo C, Hall-Jackson C, Wu R, et al. Activation of mammalian Chk1 during DNA replication arrest: a role for Chk1 in the intra-S phase checkpoint monitoring replication origin firing. J Cell Biol 2001;154:913–23.
7. Blomberg I, Hoffmann I. Ectopic expression of Cdc25A accelerates the G_1/S transition and leads to premature activation of cyclin E- and cyclin A-dependent kinases. Mol Cell Biol 1999;19:6183–94.
8. Sanchez Y, Wong C, Thoma RS, et al. Conservation of the Chk1 checkpoint pathway in mammals: linkage of DNA damage to Cdk regulation through Cdc25. Science (Wash DC) 1997;277:1497–501.
9. Kumagai A, Dunphy WG. The cdc25 protein controls tyrosine dephosphorylation of the cdc2 protein in a cell-free system. Cell 1991;64:903–14.
10. Mailand N, Podtelejnikov AV, Groth A, et al. Regulation of G_2/M events by Cdc25A through phosphorylation-dependent modulation of its stability. EMBO J 2002;21:5911–20.
11. Chen MS, Hurov J, White LS, Woodford-Thomas T, Piwnica-Worms H. Absence of apparent phenotype in mice lacking Cdc25C protein phosphatase. Mol Cell Biol 2001;21:3853–61.
12. Dixon H, Norbury CJ. Therapeutic exploitation of checkpoint defects in cancer cells lacking p53 function. Cell Cycle 2002;1:362–8.
13. Yao SL, Akhtar AJ, McKenna KA, et al. Selective radiosensitization of p53-deficient cells by caffeine-mediated activation of p34cdc2 kinase. Nat Med 1996;2:1140–3.
14. Koniaras K, Cuddihy AR, Christopoulos H, Hogg A, O'Connell MJ. Inhibition of Chk1-dependent G_2 DNA damage checkpoint radiosensitizes p53 mutant human cells. Oncogene 2001;20:7453–63.
15. Sarkaria JN, Busby EC, Tibbetts RS, et al. Inhibition of ATM and ATR kinase activities by the radiosensitizing agent, caffeine. Cancer Res 1999;59:4375–82.
16. Rowley R, Zorch M, Leeper DB. Effect of caffeine on radiation-induced mitotic delay: delayed expression of G_2 arrest. Radiat Res 1984;97:178–85.
17. Graves PR, Yu L, Schwarz JK, et al. The Chk1 protein kinase and the Cdc25C regulatory pathways are targets of the anticancer agent UCN-01. J Biol Chem 2000;275:5600–5.
18. Iliakis G, Wang Y, Guan J, Wang H. DNA damage checkpoint control in cells exposed to ionizing radiation. Oncogene 2003;22:5834–47.
19. Xu B, Kim ST, Lim DS, Kastan MB. Two molecularly distinct G_2/M checkpoints are induced by ionizing irradiation. Mol Cell Biol 2002;22:1049–59.
20. Wang H, Boecker W, Wang X, et al. Caffeine inhibits homology-directed repair of I-SceI-induced DNA double-strand breaks. Oncogene 2004;23:824–34.
21. Bernhard EJ, Muschel RJ, Bakanauskas VJ, McKenna WG. Reducing the radiation-induced G_2 delay causes HeLa cells to undergo apoptosis instead of mitotic death. Int J Radiat Biol 1996;69:575–84.
22. Puck TT, Marcus PI. Action of x-rays on mammalian cells. J Exp Med 1956;103:653–66.
23. Ianzini F, Mackey MA. Spontaneous premature chromosome condensation and mitotic catastrophe following irradiation of HeLa S3 cells. Int J Radiat Biol 1997;72:409–21.
24. Muller WU, Schlusen I, Streffer C. Direct evidence that radiation induced micronuclei of early embryos require a mitosis for expression. Radiat Environ Biophys 1991;30:117–22.
25. Jonathan EC, Bernhard EJ, McKenna WG. How does radiation kill cells? Curr Opin Chem Biol 1999;3:77–83.
26. Dewey WC, Ling CC, Meyn RE. Radiation-induced apoptosis: relevance to radiotherapy. Int J Radiat Oncol Biol Phys 1995;33:781–96.
27. Forrester HB, Albright N, Ling CC, Dewey WC. Computerized video time-lapse analysis of apoptosis of REC:Myc cells X-irradiated in different phases of the cell cycle. Radiat Res 2000;154:625–39.
28. Dikomey E, Borgmann K, Brammer I, Kasten-Pisula U. Molecular mechanisms of individual radiosensitivity studied in normal diploid human fibroblasts. Toxicology 2003;193:125–35.
29. Fehrenbacher N, Gyrd-Hansen M, Poulsen B, et al. Sensitization to the lysosomal cell death pathway upon immortalization and transformation. Cancer Res 2004;64:5301–10.
30. Sato N, Mizumoto K, Nakamura M, et al. A possible role for centrosome overduplication in radiation-induced cell death. Oncogene 2000;19:5281–90.
31. Kanda T, Sullivan KF, Wahl GM. Histone-GFP fusion protein enables sensitive analysis of chromosome dynamics in living mammalian cells. Curr Biol 1998;8:377–85.
32. Earnshaw WC. Nuclear changes in apoptosis. Curr Opin Cell Biol 1995;7:337–43.
33. Galgoczy DJ, Toczyski DP. Checkpoint adaptation precedes spontaneous and damage-induced genomic instability in yeast. Mol Cell Biol 2001;21:1710–8.
34. Yoo HY, Kumagai A, Shevchenko A, Dunphy WG. Adaptation of a DNA replication checkpoint response depends upon inactivation of claspin by the Polo-like kinase. Cell 2004;117:575–88.
35. Chu K, Leonhardt EA, Trinh M, et al. Computerized video time-lapse (CVTL) analysis of cell death kinetics in human bladder carcinoma cells (EJ30) X-irradiated in different phases of the cell cycle. Radiat Res 2002;158:667–77.
36. Den Elzen N, Kosoy A, Christopoulos H, O'Connell MJ. Resisting arrest: recovery from checkpoint arrest through dephosphorylation of Chk1 by PP1. Cell Cycle 2004;3:529–33.
37. Shiloh Y. ATM and related protein kinases: safeguarding genome integrity. Nat Rev Cancer 2003;3:155–68.
38. Ford MD, Martin L, Lavin MF. The effects of ionizing radiation on cell cycle progression in ataxia telangiectasia. Mutat Res 1984;125:115–22.
39. Beamish H, Lavin MF. Radiosensitivity in ataxia-telangiectasia: anomalies in radiation-induced cell cycle delay. Int J Radiat Biol 1994;65:175–84.
40. Hlatky L, Sachs RK, Vazquez M, Cornforth MN. Radiation-induced chromosome aberrations: insights gained from biophysical modeling. Bioessays 2002;24:714–23.
41. Forrester HB, Vidair CA, Albright N, Ling CC, Dewey WC. Using computerized video time lapse for quantifying cell death of X-irradiated rat embryo cells transfected with c-myc or c-Ha-ras. Cancer Res 1999;59:931–9.
42. Monks A, Harris ED, Vaigro-Wolff A, et al. UCN-01 enhances the in vitro toxicity of clinical agents in human tumor cell lines. Investig New Drugs 2000;18:95–107.
43. Wang Q, Fan S, Eastman A, et al. UCN-01: a potent abrogator of G_2 checkpoint function in cancer cells with disrupted p53. J Natl Cancer Inst (Bethesda) 1996;88:956–65.
44. Hirose Y, Berger MS, Pieper RO. Abrogation of the Chk1-mediated G_2 checkpoint pathway potentiates temozolomide-induced toxicity in a p53-independent manner in human glioblastoma cells. Cancer Res 2001;61:5843–9.

Downloaded from cancerres.aacrjournals.org on September 18, 2021. © 2004 American Association for Cancer Research.

AACR American Association for Cancer Research

Cancer Research
The Journal of Cancer Research (1916–1930) | The American Journal of Cancer (1931–1940)

Inhibition of Chk1 by CEP-3891 Accelerates Mitotic Nuclear Fragmentation in Response to Ionizing Radiation

Randi G. Syljuåsen, Claus Storgaard Sørensen, Jesper Nylandsted, et al.

Cancer Res 2004;64:9035-9040.

Updated version	Access the most recent version of this article at: http://cancerres.aacrjournals.org/content/64/24/9035
Supplementary Material	Access the most recent supplemental material at: http://cancerres.aacrjournals.org/content/suppl/2005/01/14/64.24.9035.DC1

Cited articles	This article cites 44 articles, 17 of which you can access for free at: http://cancerres.aacrjournals.org/content/64/24/9035.full#ref-list-1
Citing articles	This article has been cited by 28 HighWire-hosted articles. Access the articles at: http://cancerres.aacrjournals.org/content/64/24/9035.full#related-urls

E-mail alerts	Sign up to receive free email-alerts related to this article or journal.
Reprints and Subscriptions	To order reprints of this article or to subscribe to the journal, contact the AACR Publications Department at pubs@aacr.org.
Permissions	To request permission to re-use all or part of this article, use this link http://cancerres.aacrjournals.org/content/64/24/9035. Click on "Request Permissions" which will take you to the Copyright Clearance Center's (CCC) Rightslink site.

Downloaded from cancerres.aacrjournals.org on September 18, 2021. © 2004 American Association for Cancer Research.